

Observing Long Cosmic Strings Through Gravitational Lensing

Andrew A. de Laix

Case Western Reserve University, Department of Physics, Cleveland Ohio, 44106-7079

(August 18, 2018)

We consider the gravitational lensing produced by long cosmic strings formed in a GUT scale phase transition. We derive a formula for the deflection of photons which pass near the strings that reduces to an integral over the light cone projection of the string configuration plus constant terms which are not important for lensing. Our strings are produced by performing numerical simulations of cosmic string networks in flat, Minkowski space ignoring the effects of cosmological expansion. These strings have more small scale structure than those from an expanding universe simulation—fractal dimension 1.3 for Minkowski versus 1.1 for expanding—but share the same qualitative features. Lensing simulations show that for both point-like and extended objects, strings produce patterns unlike more traditional lenses, and, in particular, the kinks in strings tend to generate demagnified images which reside close to the string. Thus lensing acts as a probe of the small scale structure of a string. Estimates of lensing probability suggest that for string energy densities consistent with string seeded structure formation, on the order of tens of string lenses should be observed in the Sloan Digital Sky Survey quasar catalog. We propose a search strategy in which string lenses would be identified in the SDSS quasar survey, and the string nature of the lens can be confirmed by the observation of nearby high redshift galaxies which are also lensed by the string.

I. INTRODUCTION

The current understanding of the formation of large scale structure presumes that clusters, walls, filaments, etc. result from the gravitational collapse of small deviations from homogeneity in the early universe, but the source of these fluctuations is, at present, still a mystery. The most popular model is inflation, where vacuum energy in the early universe drives a period of exponential growth which stretches small quantum mechanical fluctuations to macroscopic scales much greater than the horizon at that time. As the universe expands, these fluctuations fall back into the causal horizon and collapse into the structure we see today. However, there is yet no definitive evidence in either accelerator experiments or cosmological observations to prove that a field with the appropriate characteristics exists to induce such an inflationary epoch. It is worthwhile, then, to consider alternatives to inflation which can also explain the origin of structure, specifically, topological defects. During cosmological phase transitions, topological defects can form where adjacent fields take on different vacuum states which can only be continuously connected if a region of false vacuum is trapped between them. The energy trapped in these defects can then gravitationally induce perturbations which will collapse into the observed structure. A particularly interesting subclass of defect models is cosmic strings, which are lineal structures formed when a $U(1)$ symmetry is spontaneously broken. If these strings were formed at the GUT scale, they can have sufficient energy, and therefore mass, to drive the necessary perturbations in the ordinary matter which collapse into the structure we observe today. The question then becomes, how can we observe strings and compare these models with inflation? Inflationary models may best be tested by microwave background observations, as these models make precise predictions for the spectrum of microwave perturbations from 180° scales down to several orders of magnitude smaller. For string models, things are less certain. On large scales, strings predict a spectrum similar enough to inflation as to be statistically indistinguishable [1]. On smaller scales, issues like decoherence [2], which smooth the acoustic peaks, are not fully understood, and while it is likely that we could rule out inflation if strings are the true model, we may not be able to confirm the existence of strings through microwave observations, given the current uncertainty about the CMBR fluctuations they produce. In this paper, we shall discuss another method by which cosmic strings can be observed, namely through gravitational lensing. Unlike other defect models, where we expect perhaps only one defect to remain in a horizon volume, simulations suggest that a significant length of string is observable today. The gravitational fluctuations these strings induce will bend light, making it possible to observe a cosmic string if it is back lit by a visible source. Since there are many sources, including galaxies and quasars, which can light up a string, we will consider the structure of images that would arise in such lensing systems containing long cosmic string. Our estimates of the string lensing probability suggest that string lenses occur at a rate of 10% to 30% of that of galaxy lenses in the case of quasar sources, a few dozen of which have been observed. We show that the resulting images have a unique signature, that is, along with the image pair

arXiv:astro-ph/9705223v1 28 May 1997

that is associated with infinite straight strings, there will usually be a series of smaller, demagnified images which reside closer to the string itself. We conclude that new quasar surveys with large angular sky coverage, like the Sloan Digital Sky Survey, should contain a significant number of string lenses and be able to definitively observe or rule out the cosmic string model, at least for flat space.

This paper is organized into several sections. In the following, we estimate the lensing probability for long cosmic strings and compare it to that for galaxies. In §III we calculate the deflection of a photon in the presence of a long cosmic string. In §IV, we discuss the basic theory of gravitational lenses. The next section is broken into two parts, where §VA discusses the generation of the long strings used in our calculations and §VB explains how these were used to find lensed images. Finally, in §VI we discuss our results and suggest a search strategy for finding string lenses.

II. LONG STRING LENSING PROBABILITY

We begin by considering the likelihood observing a string lens system. Quasars represent the best objects for seeing long string lensing, as they are bright, with images not likely to be lost in any background, and new surveys like the Sloan Digital Sky Survey will observe them in large numbers (on the order of 10^5 quasars over 1/4 of the sky). We would like to know how many quasar–string lensing systems we can expect to observe in such a survey, but this depends on how a particular quasar sample is observed. A simpler calculation is to measure the optical depth for lensing, that is the probability of an object at a given redshift being lensed, which we can then compare to optical depths for quasar–galaxy lensing, which has already been observed for about a dozen systems and should occur on the order of hundreds of cases in the SDSS.

To estimate the string lensing probability, we require two pieces of information: the projected angular density of string and a lensing cross section for that string. With regards to the former, numerical simulations of string networks in an expanding universe can give reliable estimates of the string density ρ_{ls} in a horizon volume, characterized by the horizon radius d_H . Using the results of Bennett and Bouchet [3] as a representative example, we see that in the matter dominated epoch the length of string in horizon units is a constant given by

$$L_{ls} = \frac{\rho_{ls} d_H^2}{\mu} = 31 \pm 7, \quad (1)$$

where μ is the energy per unit length of string. We shall treat this string as an ensemble of small links, with length L_l in horizon units, distributed with a uniform probability density related to the above result, each with a random orientation with respect to the line of sight. These assumptions are appropriate when considering an average over many string networks. We shall also assume that each of the links is static, since we lack good information on the distribution of link velocities. In essence we are disregarding the effects of the Lorentz contraction (see next section for details), which means our estimate is probably only accurate to a factor of a few. We now subdivide space into differential volume elements such that the probability that more than one link, located by its center of mass, resides in the same volume is vanishingly small in comparison to the probability that one link resides in that volume. For the i th volume element, we find that the differential angle of sky subtended by the string is given by

$$d\Theta_i = n_i \frac{L_l d_H}{d_A} \sin(\beta_i) dV_i, \quad (2)$$

where n_i is the number of links in the volume, β_i is a random orientation angle associated with each link, and d_A is the angular diameter distance to the link

$$d_A = \frac{2}{H_0(1+z)^2} (1+z - \sqrt{1+z}), \quad (3)$$

assuming a flat, matter dominated universe. Under the same assumptions, the volume element and horizon distance can also be expressed in terms of the redshift:

$$dV = \frac{4}{H_0^3} \frac{(1+z - \sqrt{1+z})^2}{(1+z)^3 \sqrt{1+z}} dz d\Omega, \quad (4)$$

$$d_H = \frac{2}{H_0(1+z)^{3/2}}.$$

To estimate the lensing cross section, we assume that each link has the same cross section as if it were part of an infinite straight string. In this case, the angular cross section per radian of string is

$$\delta\phi = 8\pi G\mu \frac{D_{lq}}{D_q} \sin\beta. \quad (5)$$

The distances D_{lq} and D_q are respectively the angular diameter distances from the lens to the quasar and from the source to the quasar. In flat space for a source located at a redshift of z_2 and an observer located at z_1 , the general form of the angular diameter distance is given by

$$d_A(z_1, z_2) = \frac{2}{H_0(1+z_2)} \left[\frac{1}{\sqrt{1+z_1}} - \frac{1}{\sqrt{1+z_2}} \right]. \quad (6)$$

We ignore the effects of structure formation on these distances which introduce deviations from homogeneity that can affect the path length. Convolving the cross section with the angular string density, we can determine the optical depth for a quasar at a redshift of $z = z_q$:

$$\tau(z_q) = 8\pi G\mu L_l \frac{1}{\Omega_O} \sum_i n_i \sin^2(\beta_i) \frac{d_H}{d_A} \frac{D_{lq}}{D_q}, \quad (7)$$

where Ω_O is the observed fraction of sky. Taking the expectation value for τ , we find that $\langle n_i \rangle = L_{ls}/(L_l d_H^3)$ and $\langle \sin^2(\beta) \rangle = 2/3$. This leaves us with the integral over the observed volume

$$\langle \tau \rangle = \frac{16}{3} \pi G\mu L_{ls} \int \frac{dV}{\Omega_0} \frac{1}{d_A d_H^2} \frac{D_{lq}}{D_q}, \quad (8)$$

which can be performed analytically, giving the final result:

$$\tau(z_q) = \frac{8}{3} \pi G\mu L_{ls} \left[\frac{1}{21} z_q^3 + \frac{13}{105} z_q^2 + \frac{3}{35} z_q + \frac{2}{35} - \sqrt{1+z_q} \left(\frac{2}{105} z_q^2 + \frac{2}{35} z_q + \frac{2}{35} \right) \right]. \quad (9)$$

Now we would like to estimate the variance in τ which will permit us to set limits on string parameters using lensing statistics. Results from numerical simulations indicate that on scales of about $0.1d_H$, the string undergoes a random walk. To make the problem tractible, we shall continue to treat each of these segments as uncorrelated with the rest, and presume that the random walk correlation is fairly small. The mean of the square of the optical depth is given by

$$\langle \tau^2 \rangle = \frac{1}{\Omega_O^2} (8\pi G\mu L_l)^2 \sum_{i,j} \langle n_i n_j \rangle \langle \sin^2(\beta_i) \sin^2(\beta_j) \rangle \left(\frac{d_h}{d_A} \frac{D_{lq}}{D_q} \right)_i \left(\frac{d_h}{d_A} \frac{D_{lq}}{D_q} \right)_j. \quad (10)$$

The expectation value $\langle n_i n_j \rangle$ in the limit of differential volumes is equal to

$$\langle n_i n_j \rangle = n^2 dV_i dV_j + n dV_i \delta_{i,j}, \quad (11)$$

when n_i and n_j are uncorrelated, and $n = \langle n_i \rangle$. Given this relation, one can easily show that

$$\sigma_\tau^2 = \langle \tau^2 \rangle - \langle \tau \rangle^2 = \frac{1}{\Omega_O^2} (8\pi G\mu L_{ls})^2 \frac{L_l}{L_{ls}} \int dV \frac{8}{15} \frac{1}{d_H d_A^2} \left(\frac{D_{lq}}{D_q} \right)^2, \quad (12)$$

which has the analytic result

$$\sigma_\tau^2 = \frac{1}{\Omega_O} (8\pi G\mu L_{ls})^2 \frac{L_l}{L_{ls}} \frac{2}{225} \frac{z_q^3 + 3z_q^2 - 12z_q - 24 + 24\sqrt{1+z_q}}{(\sqrt{1+z_q} - 1)^2}. \quad (13)$$

To get the full error in τ we convolve this result with the theoretical uncertainty in the long string density σ_{ls} given in eq. (1), which adds in quadrature. Now consider a distribution of sources with mean number density as a function of redshift $N(z)$. The expected number of observed lenses is given simply by

$$\int dV N(z) \tau(z). \quad (14)$$

To calculate the variance, we must account for both the variance in τ and the Poisson fluctuations in the source distribution. Including both these effects, we find the full variance is

$$\sigma^2 = \int dV \left(N(z)\tau(z) + N(z)^2\sigma_\tau^2(z) + N(z)^2\tau^2(z)\frac{\sigma_{ls}^2}{L_{ls}} \right). \quad (15)$$

As a toy example, we consider a quasar distribution given by $N(z) = \delta(z-2)10^5/\pi$, which rough approximates that of the Sloan Digital Sky Survey. The SDSS will observe one quarter of the full sky, so using the results of this section, we find for $G\mu = 10^{-6}$, that the number of observed quasar lenses is 18 ± 6 .

In figure 1 we show the optical depth for long cosmic strings, assuming a value $G\mu = 10^{-6}$, compared with the optical depth resulting from galaxy lenses as calculated by Turner, Ostriker, and Gott [4]. The galaxy estimate is based on an isothermal sphere model, which represent an upper limit to the lensing probability, as including a finite core to the galaxy tends to reduce the optical depth by up to 50% [5]. Thus we expect that for a wide field survey anywhere from 10% to 30% of the observed lenses will be the result of long cosmic strings when compared to galaxy lenses (assuming $G\mu = 10^{-6}$). Given that order 10 quasar lensed have been observed, one may expect that a few string lenses should have been seen. In fact there are no lenses that have yet been ascribed to cosmic strings, but this is statistically unsurprising because of the large variance associated with small number statistics. We can, however, reasonably conclude that string tensions $G\mu$ greater than a few 10^{-6} , which would predict tens of observed lenses, probably are ruled out, consistent with the limits from pulsar timing.

III. GEODESIC DEFLECTION BY A LONG COSMIC STRING

In a previous paper [6], we derived an equation for the deflection of a null geodesic—corresponding to a photon trajectory in the geometric limit—arising from the gravitational field of a cosmic string loop. For long cosmic strings, we can make use of some of that derivation, but we must now be careful, as the long strings stretch to horizon scales, requiring us to consider certain surface terms which could safely be ignored when examining small loops. Let us begin again by assuming a weak field so that the full metric may be expressed as

$$g_{\mu\nu} = \eta_{\mu\nu} + h_{\mu\nu}, \quad (16)$$

where $\eta_{\mu\nu} = \text{diag}(-1, 1, 1, 1)$ is the usual Minkowski metric and $h_{\mu\nu}$ is a small perturbation such that all terms of $O(h^2)$ are negligible. For simplicity, we choose to work in the harmonic gauge, which implies the condition $g_{\mu\nu}\Gamma_{\mu\nu}^\lambda = 0$. Using this gauge choice, to linear order we are left with a simple wave equation for the metric

$$\square^2 h_{\mu\nu} = -16\pi G S_{\mu\nu}, \quad (17)$$

where $S_{\mu\nu} = T_{\mu\nu} - 1/2\eta_{\mu\nu}T_\lambda^\lambda$ is the traceless component of the stress energy tensor $T_{\mu\nu}$. If we decompose the photon four velocity γ^μ into its zeroth and first order pieces, $\gamma_{(0)}^\mu$ and $\gamma_{(1)}^\mu$ respectively, then it is a straightforward calculation to solve the geodesic equation and show that the first order deflection for a photon emitted at t_1 and observed at t_2 is given by

$$\gamma_{\alpha(1)} = \frac{1}{2} \int_{t_1}^{t_2} dt h_{\mu\nu,\alpha} \gamma_{(0)}^\mu \gamma_{(0)}^\nu - h_{\mu\alpha} \gamma_{(0)}^\mu \Big|_{t_1}^{t_2}, \quad (18)$$

Where we are integrating over the photons zeroth order trajectory, *i.e.* $x_\mu = x_{\mu 0} + \gamma_{\mu(0)} t$. For loops, which are compact, we could safely ignore the second surface term, but for now we should retain it when considering long cosmic strings as they are not compact objects.

To make further progress, we need to consider the form of the stress energy tensor resulting from a cosmic string. Strings are well approximated as lineal gravitational sources, so the string configuration at any time is given by a two parameter vector function $\mathbf{f}(\sigma, t)$ where t is the time and σ is a parameter which runs along the conformal length of the string. One may straight forwardly infer from this that the string traceless stress energy may be written in the form

$$S_{\mu\nu} = \mu \int d\sigma F_{\mu\nu} \delta^{(3)}(\mathbf{x} - \mathbf{f}(\sigma, t)), \quad (19)$$

Where μ is again the string energy density and $F_{\mu\nu}$ can be expressed in terms of \mathbf{f} and its derivatives. Now, let us designate $\tilde{\gamma}_\alpha$ to be the contribution to the first order deflection which comes from the integral in eq. (18), separating it from the surface term. Contracting this with a derivative, we get

$$\begin{aligned}
\partial^\alpha \tilde{\gamma}_\alpha &= \frac{1}{2} \int_{t_1}^{t_2} dt \square^2 h_{\mu\nu} \gamma_{(0)}^\mu \gamma_{(0)}^\nu \\
&= -8\pi G \int_{t_1}^{t_2} dt S_{\mu\nu} \gamma_{(0)}^\mu \gamma_{(0)}^\nu,
\end{aligned} \tag{20}$$

where the second line comes from the metric equation (17). Plugging in the stress energy from eq. (19), we see that

$$\partial^\alpha \tilde{\gamma}_\alpha = -8\pi G \mu \int d\sigma \int_{t_1}^{t_2} dt F_{\mu\nu} \delta^{(3)}(\mathbf{x}_0 + \boldsymbol{\gamma}_{(0)} t - \mathbf{f}(\sigma, t)) \gamma_{(0)}^\mu \gamma_{(0)}^\nu. \tag{21}$$

We can evaluate the time integral if we decompose \mathbf{f} into components which are perpendicular, \mathbf{f}_\perp , and parallel, \mathbf{f}_\parallel , to the zeroth order photon trajectory, with the result

$$\partial^\alpha \tilde{\gamma}_\alpha = -8\pi G \mu \int d\sigma \left[\frac{F_{\mu\nu} \gamma_{(0)}^\mu \gamma_{(0)}^\nu}{1 - \dot{f}_\parallel} \delta^{(2)}(\mathbf{x}_{\perp 0} - \mathbf{f}_\perp) \right]_{t=t_0}, \tag{22}$$

where t_0 is the solution to the equation $t_0 = f_\parallel(\sigma, t_0) - x_{\parallel 0}$, *i.e.* the light cone time slice, and dots refer to derivatives with respect to time. Note that the limits on the σ integral are constrained to the regions where a solution with $t_1 < t_0 < t_2$ exists. Now we shall write out the left hand side of the equality in terms of a parallel and perpendicular gradients, $\partial^\alpha \tilde{\gamma}_{\alpha(1)} = \nabla_\perp \cdot \tilde{\boldsymbol{\gamma}}_{\perp(1)} + \nabla_\parallel \cdot \tilde{\boldsymbol{\gamma}}_{\parallel(1)}$, where the parallel gradient can be written as $\nabla_\parallel \cdot \tilde{\boldsymbol{\gamma}}_{\parallel(1)} = \gamma_{\delta(0)} \gamma_{(0)}^\beta \partial^\delta \tilde{\gamma}_{\beta(1)}$. Now we consider the contraction $\gamma_{(0)}^\beta \tilde{\gamma}_{\beta(1)}$, which from eq. (18) is

$$\begin{aligned}
\gamma_{(0)}^\beta \gamma_{\beta(1)} &= \frac{1}{2} \int_{t_1}^{t_2} dt \gamma_{(0)}^\beta h_{\mu\nu, \beta} \gamma_{(0)}^\mu \gamma_{(0)}^\nu \\
&= \frac{1}{2} \int_{t_1}^{t_2} dt \frac{d}{dt} h_{\mu\nu} \gamma_{(0)}^\mu \gamma_{(0)}^\nu \\
&= \frac{1}{2} h_{\mu\nu} \gamma_{(0)}^\mu \gamma_{(0)}^\nu \Big|_{t_1}^{t_2}.
\end{aligned} \tag{23}$$

We are able to perform this integration because $\gamma_{(0)}^\beta \partial_\beta$ is equivalent to taking a complete derivative with time, d/dt . Using the above result in conjunction with eq. (22), it is easy to show

$$\nabla_\perp \cdot \tilde{\boldsymbol{\gamma}}_{\perp(1)} = -8\pi G \mu \int d\sigma \left[\frac{F_{\mu\nu} \gamma_{(0)}^\mu \gamma_{(0)}^\nu}{1 - \dot{f}_\parallel} \delta^{(2)}(\mathbf{x}_{\perp 0} - \mathbf{f}_\perp) \right]_{t=t_0} - \frac{1}{2} \frac{d}{dt} h_{\mu\nu} \gamma_{(0)}^\mu \gamma_{(0)}^\nu \Big|_{t_1}^{t_2}. \tag{24}$$

We can solve this equation by assuming that the first order deflection can be written as a gradient of a potential, $\tilde{\boldsymbol{\gamma}}_{\perp(1)} = \nabla_\perp \Phi$, leaving a two dimensional Poisson equation from which Φ may be found by integrating over the Greens function for the two dimensional Laplacian, $G(\mathbf{x}_\perp, \mathbf{x}'_\perp) = -\ln(|\mathbf{x}'_\perp - \mathbf{x}_{\perp 0}|^2)/4\pi$. Specifically, we get

$$\begin{aligned}
\Phi &= \frac{1}{8\pi} \int d^2 x'_\perp \ln(|\mathbf{x}_{\perp 0} - \mathbf{x}'_\perp|^2) \frac{d}{dt} h_{\mu\nu}(\mathbf{x}'_\perp + \mathbf{x}_{\parallel 0} + \boldsymbol{\gamma} t, t) \gamma_{(0)}^\mu \gamma_{(0)}^\nu \Big|_{t_1}^{t_2} \\
&\quad - 2G\mu \int d\sigma \left[\frac{F_{\mu\nu} \gamma_{(0)}^\mu \gamma_{(0)}^\nu}{1 - \dot{f}_\parallel} \ln(|\mathbf{f}_\perp - \mathbf{x}_{\perp 0}|^2) \right]_{t=t_0}.
\end{aligned} \tag{25}$$

Finally, to recover the perpendicular deflection, we take the gradient and add the surface term from eq. (18) which leaves us with

$$\begin{aligned}
\boldsymbol{\gamma}_\perp &= \frac{1}{4\pi} \int d^2 x'_\perp \frac{\mathbf{x}_{\perp 0} - \mathbf{x}'_\perp}{|\mathbf{x}_{\perp 0} - \mathbf{x}'_\perp|^2} \frac{d}{dt} h_{\mu\nu}(\mathbf{x}'_\perp + \mathbf{x}_{\parallel 0} + \boldsymbol{\gamma} t, t) \gamma_{(0)}^\mu \gamma_{(0)}^\nu \Big|_{t_1}^{t_2} \\
&\quad + 4G\mu \int d\sigma \left[\frac{F_{\mu\nu} \gamma_{(0)}^\mu \gamma_{(0)}^\nu}{1 - \dot{f}_\parallel} \frac{\mathbf{f}_\perp - \mathbf{x}_{\perp 0}}{|\mathbf{f}_\perp - \mathbf{x}_{\perp 0}|^2} \right]_{t=t_0} - \mathbf{h}_\perp \Big|_{t_1}^{t_2}.
\end{aligned} \tag{26}$$

where \mathbf{h}_\perp is defined to be the perpendicular part of $h_{\mu\alpha}\gamma_{(0)}^\mu$. This result gives us exactly what we want for lensing calculations, the photon deflection away from its zeroth order path. The values of γ_0 and γ_\parallel which are equivalent to first order, give us the redshift of a photon as it passes a string, but we are not interested in this calculation here.

Eq. (26) may at first seem to be a retrograde step as it involves a two dimensional integral of the metric in space where originally we had only a one dimensional integral of the metric over time. However, we argue that the first and third terms which contain the metric explicitly can be neglected. To do so we require an explicit solution for the metric in terms of the stress energy:

$$h_{\mu\nu}(\mathbf{x}, t) = 4G \int d^3x' \frac{S_{\mu\nu}(\mathbf{x}', \tau)}{|\mathbf{x} - \mathbf{x}'|}, \quad (27)$$

where $\tau = t - |\mathbf{x} - \mathbf{x}'|$ is the retarded time, and this solution is derived from the Greens function for the \square^2 operator. Using our string stress energy given in eq. (19), we can reduce the metric to

$$h_{\mu\nu}(\mathbf{x}, t) = 4G\mu \int d\sigma \frac{F_{\mu\nu}(\sigma, \tau)}{|\mathbf{x} - \mathbf{f}| - (\mathbf{x} - \mathbf{f}) \cdot \dot{\mathbf{f}}}. \quad (28)$$

Now consider points which are far from the string. The metric goes like an integral over $|\mathbf{x} - \mathbf{f}|^{-1}$ while the middle term in eq. (26) goes like an integral over $|\mathbf{x}_{\perp 0} - \mathbf{f}_\perp|^{-1}$. The latter represents the minimum distance between the zeroth order photon trajectory and the cosmic string, while the former will, in general, go like the distance from the photon to the string at the current time. In the case of string loops, we could expect that the two metric terms would fall off like the inverse of the distance while the middle term remained constant, thus allowing us to drop the explicit metric terms. With an infinite string, one must be more careful because the distance from the string can never be large with respect to the string size. However, when determining the image structure in lensing, it is not the absolute deflection of the photons which matters, but rather, it is the difference in deflection between two nearby rays that counts. In this case, we see that for photons far from the string, the difference in the contribution between the two metric terms declines with distance while the difference between the static terms remains constant. So, for photons which pass nearby the string, that is a small distance when compared to the source and observer, the effect of the metric terms then is merely to cause all of the images to be displaced, but not to alter the shape or relative orientation of the images. Thus, for the purposes of determining the structure of strong lensing due to strings, we may drop the explicit metric terms all together and write

$$\gamma_\perp = 4G\mu \int d\sigma \left[\frac{F_{\mu\nu}\gamma_{(0)}^\mu\gamma_{(0)}^\nu}{1 - \dot{f}_\parallel} \frac{\mathbf{f}_\perp - \mathbf{x}_{\perp 0}}{|\mathbf{f}_\perp - \mathbf{x}_{\perp 0}|^2} \right]_{t=t_0}, \quad (29)$$

where the omitted terms only add a constant to this result when the photon impact parameter is small compared to the distances of the source and observer to the lens.

IV. BASIC GRAVITATIONAL LENSING THEORY

Before we consider the specific example of a long cosmic string lens, let us first take a detour into the basic theory of gravitational lensing. For most calculations, it is more than adequate to consider photon trajectories as the path taken by null geodesics like those discussed in the previous section, so that the lensing system is described by simple geometry and wave properties are ignored. In figure 2 we show a pictorial representation of a gravitational lensing system with an optical axis defined to roughly intersect the center of the lens. A photon is emitted from a source S displaced from the optical axis by a vector $\boldsymbol{\eta}$ at a distance of D_s from an observer and D_{ls} from the lens, and it travels in a straight line until it reaches the plane of the lens. There, its trajectory is deflected by a vector $\bar{\boldsymbol{\alpha}}$, defined as the initial trajectory minus the final, and it again travels in a straight line to the observer located at a distance D_l from the lens. This approximation is known as the thin lens approximation because the lens and the deflection it induces are presumed to occur in a single plane. To first order, this is valid for long cosmic strings. The location of the image I , where the ray intersects the lens plane, defines the vector $\boldsymbol{\xi}$ which is measured from the the optical axis to I in the lens plane. Since we will be considering sources and observers that are separated on cosmological scales, The distances D_l , D_{ls} and D_s are angular diameter distances (see eq. (6)).

In the small angle limit, the condition that a ray emitted from the source will have an image seen at I by an observer at O requires that

$$\boldsymbol{\eta} = \frac{D_s}{D_l} \boldsymbol{\xi} - D_{ls} \bar{\boldsymbol{\alpha}}(\boldsymbol{\xi}). \quad (30)$$

This equation, often referred to as the lens equation, gives one the unique source location for any observed image, but its inverse, however, is not unique, as a single source may generate more than one image. It is convenient to recast the lens equation into a dimensionless form by dividing through by the length D_l , so that the coordinates are given in units of angular displacement with respect to the optical axis. Thus we define a new set of variables

$$\mathbf{x} \equiv \frac{\boldsymbol{\xi}}{D_l}, \quad (31)$$

$$\mathbf{y} \equiv \frac{\boldsymbol{\eta}}{D_s},$$

$$\boldsymbol{\alpha} \equiv \bar{\boldsymbol{\alpha}} \frac{D_{ls}}{D_s}, \quad (32)$$

which yield a dimensionless lens equation

$$\mathbf{y} = \mathbf{x} - \boldsymbol{\alpha}(\mathbf{x}). \quad (33)$$

The above equation can be inverted to give the location of images for a particular source location, but one can also use the information contained therein to determine the magnification of those images. Suppose a source emits a narrow pencil beam of photons which subtends a solid angle $d\Omega^*$, while the image of the source beam subtends an angle $d\Omega$, so that the ratio of the solid angles $d\Omega^*/d\Omega$ will give the flux magnification of the image to the source. Using the lens equation, one can derive the magnification by considering the Jacobian matrix

$$A_{ij} = \frac{\partial y_i}{\partial x_j}, \quad (34)$$

and observing that the magnification factor $\mathcal{M}(\mathbf{x}) = d\Omega^*/d\Omega(\mathbf{x})$ is given by the inverse of the determinant of A_{ij} ,

$$\mathcal{M}(\mathbf{x}) = \frac{1}{\det A(\mathbf{x})}. \quad (35)$$

Note that this same factor will give the angular magnification for extended objects, so gravitational lenses conserve surface brightness.

V. NUMERICAL CALCULATIONS WITH LONG STRINGS

A. Constructing Long String Networks

In §III, we derived an expression for the photon deflection that will be relevant to gravitational lensing with cosmic strings; now we must consider the problem of generating realistic long cosmic strings. Analytic work, in particular scaling solutions, has successfully described some of the average properties of long strings, but it cannot give the details of the structure of a particular string. Only by simulating networks of interacting strings can we hope to generate realistic structure. This exercise can be greatly simplified if we restrict ourselves to flat, Minkowski space rather than considering the expanding universe, but the resulting structure of these strings will not quantitatively agree with those produced by expanding universe models. However, there should be good qualitative agreement, sufficient for our lensing analysis. That is, we expect that the structure of the lensed images should be similar enough to those which would result from more accurate string simulations to make general conclusions about string lenses.

Let us begin by considering the equations of motion for a cosmic string. The dynamics of strings are dominated by their tension, while gravitational effects are suppressed by factors of order $G\mu$, so for now we can ignore the back reaction, but we will discuss its effects later. We need the string location which is described by a four vector f^μ with a time like component $f^0 = t$ and spatial displacement $\mathbf{f}(\sigma, t)$ that we used in the previous section. Then, considering only tension, the equations of motion for the string are

$$\ddot{f}^\mu - f''^\mu = 0, \quad (36)$$

where dots refer to derivatives with respect to time and primes refer to derivatives with respect to σ . Our choice of the harmonic gauge enforces two constraints,

$$\dot{f}^\mu f'_\mu = 0 \quad (37)$$

and

$$\dot{f}^2 + f'^2 = 0, \quad (38)$$

which restrict the motion to transverse directions and mandate conservation of energy respectively. The stress energy can also be expressed as a function of \mathbf{f} and has the form

$$T_{\mu\nu} = \mu \int d\sigma (\dot{f}_\mu \dot{f}_\nu - f'_\mu f'_\nu) \delta^{(3)}(\mathbf{x} - \mathbf{f}(\sigma, t)), \quad (39)$$

consistent with the form suggested in eq. (19).

For non-interacting strings, it would be sufficient to specify some initial conditions consistent with the gauge constraints and evolve them using the wave equation. However, real strings can interact when two different segments intersect, causing them to reconnect with the opposite segment. To handle both the evolution and intersection of the string network, we shall turn to a clever algorithm first proposed by Smith and Villenkin [7]. The foundation of the Smith–Villenkin algorithm is the fact that for a set of points equally spaced in σ , separated by δ , the wave equation (36) can be reduced exactly to a finite difference equation on a lattice of σ and t points. In terms of the displacement vector \mathbf{f} , we get

$$\mathbf{f}(\sigma, t + \delta) = \mathbf{f}(\sigma + \delta, t) + \mathbf{f}(\sigma - \delta, t) - \mathbf{f}(\sigma, t - \delta) \quad (40)$$

This second order equation can be reduced to a pair of first order equations if we consider the velocity, defined as

$$\dot{\mathbf{f}} \equiv \left\{ \mathbf{f}(\sigma, t + \delta) - \frac{1}{2} [\mathbf{f}(\sigma + \delta, t) + \mathbf{f}(\sigma - \delta, t)] \right\} / \delta. \quad (41)$$

Thus, we get

$$\mathbf{f}(\sigma, t + \delta) = \frac{1}{2} [\mathbf{f}(\sigma + \delta, t) + \mathbf{f}(\sigma - \delta, t)] + \dot{\mathbf{f}}(\sigma, t) \delta, \quad (42)$$

and

$$\dot{\mathbf{f}}(\sigma, t + \delta) = \frac{1}{2} [\dot{\mathbf{f}}(\sigma + \delta, t) + \dot{\mathbf{f}}(\sigma - \delta, t)] + [\mathbf{f}(\sigma + 2\delta, t) - 2\mathbf{f}(\sigma, t) + \mathbf{f}(\sigma - 2\delta, t)] / 4\delta. \quad (43)$$

A complete solution can be specified by initially fixing the positions for every even point on the σ lattice and velocities for every odd point. After the first time step, eq.'s (42 & 43) will give the positions for each odd point on the σ lattice and velocities for each even point on the lattice. After the second time step, even points will again be positions and odd points will again be velocities, and so on, so that in general, the plane of σ and t will be filled with interlocking diamond lattices of positions and velocities.

The next challenge is to satisfy the gauge constraints on the lattice. In eq. (41) we have given a discrete velocity, and now we need a discrete version for the σ derivative. It has the obvious form

$$\mathbf{f}'(\sigma, t) \equiv [\mathbf{f}(\sigma + \delta, t) - \mathbf{f}(\sigma - \delta, t)] / 2\delta, \quad (44)$$

where the gauge constraints for the discrete \mathbf{f} remain unchanged,

$$\dot{\mathbf{f}} \cdot \mathbf{f}' = 0, \quad (45)$$

and

$$\dot{\mathbf{f}}^2 + \mathbf{f}'^2 = 1. \quad (46)$$

To ensure that these conditions would be preserved through the entire evolution of the string, Smith and Villenkin proposed discretizing space in the same way as σ and t , that is, the space itself is a lattice of points with spacing δ . String configurations are then described by a series of connected links between successive string points on the σ lattice consisting of three possible types. The first type is a static link with $\dot{\mathbf{f}} = 0$ and $|\Delta\mathbf{f}| = 2$, implying that one coordinate of $\Delta\mathbf{f}$ is $\pm 2\delta$ while the others are zero. The second type is a moving link for which $|\mathbf{f}'| = |\dot{\mathbf{f}}| = \sqrt{2}/2$. Two components of $\Delta\mathbf{f}$ are $\pm\delta$ while the final is zero, and the velocity $\dot{\mathbf{f}}$ also has two non zero components which

are each $\pm 1/2$ and must be normal to $\Delta \mathbf{f}$. The last type of link is a cusp where $\Delta \mathbf{f} = 0$. The velocity of a cusp is 1 corresponding to a link traveling at the speed of light parallel to one of the axes. One can verify easily that all of these links satisfy the gauge conditions and that the constraints will be preserved by the equations of motion.

Finally, to accurately evolve a string network, we must account for string inter-commutations which occur when different segments of the string collide. We have defined links which are connections of two successive string positions $\mathbf{f}(\sigma, t)$ and $\mathbf{f}(\sigma + \delta, t)$. A collision occurs when two string points $\mathbf{f}(\sigma_i, t)$ and $\mathbf{f}(\sigma_j, t)$ both fall on the same location. If this happens, we inter-commute the links so now the point $\mathbf{f}(\sigma_i, t)$ is connected to $\mathbf{f}(\sigma_j + \delta, t)$ and the point $\mathbf{f}(\sigma_j, t)$ is connected to $\mathbf{f}(\sigma_i + \delta, t)$ with care taken to ensure that the proper velocity is assigned to each link. Prior to each time step, one tests each of the points to see if it lies in the same position as any other. One inter-commutes all the colliding links, and then evolves time for one step δ and checks the strings again for inter-commutations. To ensure that cusps are not mistaken for collisions, we set a minimum separation in σ space, 4δ , required before an inter-commutation on a distinct string is allowed. This fixes a minimum loop size, but the structure of the long strings is insensitive to the choice so long as it is small in comparison to the overall string length. In passing we mention that the order N^2 process of testing each point for intersection can be reduced to an order few $N \log N$ process if one sorts the points with respect to their positions using a quick sorting routine first.

The Smith–Villain algorithm is a powerful tool for evolving networks of cosmic strings, and now we shall consider the initial conditions which we will use to produce long string segments for gravitational lensing. We start with the standard initial conditions introduced by Vachaspati and Villain [8], who lay down a periodic lattice of phases, and locate strings through the faces of the lattice cubes which have non-zero winding number. The result is a network of strings made of static segments which are parallel to one of the axes of the box, ideally suited as initial conditions for the Smith–Villain evolution algorithm. To ensure that space discretization effects do not strongly influence the resulting strings, each of these segments was subdivided into sixteen static links 2δ long, where the overall segment length is 32δ . Tests of our simulations found that subdividing the segments with a larger number of links did not change structure of the evolved network, so spatial discretization effects have been minimized. Ideally, we would like to evolve this network until it has completely relaxed, and use the resulting long strings for our lensing calculations. Unfortunately, the periodic boundary conditions insure that there can be no net string flux through the box, meaning that given sufficient time, all of the long strings will fragment into loops leaving us nothing to study. To minimize these periodic effects, we evolve the network for a time equal to half the light crossing, *i.e.* if the box is $n\delta$ wide, we take $n/2$ time steps, each δ long. We expect scales on the box size to preserve the structure of the initial conditions, but on scales smaller than $n\delta/2$, interactions should have sufficient time to relax the system to its final state.

Previous analysis of evolved string networks has shown that the small scale structure of the surviving long strings is self-similar, that is, the structure is statistically the same on all scales well below the horizon [9]. We compare our results with our predecessors, as a consistency check. The simplest test is to measure the fractal dimension of the string defined as the exponent n such that $L \propto D^n$, where L is the mean conformal length of string measured between points separated by a distance D in physical space. For self-similar structures, n is a constant for all D , and for the particular example of a random walk string, $n = 2.0$. In figure 3 we show a log-log graph of the conformal length L plotted as a function of D for the long strings produced in a box simulation with periodic length 1024δ at times $t = 0\delta$, 256δ , and 512δ . Note that our initial segments were formed in a 32^3 box of phases and each initial segment was 32δ . We can see that for the unevolved strings that the fractal dimension is roughly uniform above the initial link scale. A linear regression of these points gives a slope of $n = 2.0$ which is what one expects from a random walk. As the simulation evolves, we see that the shorter length scales begin to relax into a new structure with a smaller fractal dimension, and by the time $t = 512\delta$, scale below $D \sim 512\delta$ have almost completely relaxed. A fit to these points gives a fractal dimension of $n = 1.3$, a result consistent with those of Sakellariadou and Villain [10], and interestingly, also consistent with the early time results of expanding universe simulations. In this last type of simulation, apparently the strings first fragment and relax on time scales that are short compared to the expansion time of the universes and then are stretched so that n falls below the initial flat space value.

B. Finding Images With Long Strings

Now that we have a network of realistic long strings to work with, we consider how to use them in gravitational lensing systems. The best approach would be to evolve a large network with very fine spatial resolution (on the order of 10^{-5} the box length, where we could associate that scale with a few times the horizon scale), and just send photons through the box. Of course, the numerical resolution required to perform such a calculation is well beyond the capacity of current computers, so as an alternative, we exploit the fractal nature of the small scale structure of the string discussed in the previous subsection. Sections of string which can fit in a box of length about half the simulation box relax into a self similar structure described by a constant fractal dimension, meaning that if we were

to magnify a small piece of this string, we would observe the same structure in proportion to the new scale. Thus, to use our long strings which are not resolved on the scales relevant to gravitational lensing, we need only rescale the string, as long as we restrict ourselves to segments which have had sufficient time to relax.

Let us be more specific about precisely how we accomplish this. From our simulations described in the previous section, we have a periodic box filled with loops and long strings. We can eliminate the loops by considering only strings which are significantly longer than the box length, leaving the long strings which tend to wrap around the box periodically once or more. It is the smaller scales, for which the string has relaxed to its final structure, that we wish to consider. To do so, we remove a long string from the box entirely, laying it end to end no longer in a periodic box. If the string wraps around the original network box more than once, we connect the the box size segments by shifting the endpoints to make one super-long string. Now we need to determine the the light cone projection of the string required to find the deflection given by eq. (26). We accomplish this by allowing our single long string to evolve independently of the network, turning off all inter-commutations and connecting the end points periodically. Inter-commutations are ignored because we do not want to alter the small structure of the string. A photon is presumed to travel along one of the axes, and the location of the intersection of each of the string points with the light cone, along with the string velocity is recorded. Since each string point is equal spaced in σ , we can use the set of light cone projected points to reduce the integral in eq. (26) to a discrete sum. We do not, however, wish to use the entire long string, since the structure has not relaxed on the largest scales. Instead, starting at an arbitrary point, we select shorter segments—those which can fit in a box with side length half that of the original network—and use only these points to calculate the photon deflection.

In truncating the summation and considering only a finite string segment, we obviously introduce errors which we would like to quantify. As a order of magnitude estimate, let us consider the special case of an finite straight string segment perpendicular to the photon trajectory with equal lengths ℓ above and below the photon axis. We consider the photon to be moving along the z axis and place the string segment parallel to the y axis a distance d from the origin (defined by the photon) so that the deflection will be along the x direction. Using eq. (29), while observing that $f_{||} = 0$ and $F_{\mu\nu}\gamma^\mu\gamma^\nu = 1$, we see that the magnitude of the deflection will be proportional to

$$\int_{-\ell}^{\ell} \frac{d}{\sigma^2 + d^2} = 2 \tan^{-1}(\ell/d), \quad (47)$$

and the truncation error, that is the difference between $\ell \rightarrow \infty$ and finite ℓ , goes as $\pi - 2 \tan^{-1}(\ell/d)$. In the limit of large ℓ this is approximately $2d/\ell$. If instead we wish to look at a fractal string, then we should replace the σ^2 in the integral with something proportional to $\sigma^{2/n}$ which gives a truncation error which falls like $(d/\ell)^{(2/n)-1}$. So, we see that the error depends on how far the photon passes from the string, which is fortuitous since most of the interesting lensing occurs for photons which pass close to the string segment. We can also see that the thin lens approximation is justified. So long as d is much smaller than the distances of the source and observer from the lens, $\sim D$, then the deflection will occur in a region within a few lengths d from the string which, and including the effects arising from the non-instantaneous deflection would be second order in d/D .

Given the projected string segment, we have everything necessary to examine gravitational lensing, but now the challenge is to solve the lens equation. Currently there is no fast way to invert a multidimensional equation like eq. (33), so our only choice is to solve the problem by brute force. Given a source and lens redshift, we calculate the deflection $\alpha(\mathbf{x})$ on a uniform grid in \mathbf{x} space, and then use the lens equation to solve for \mathbf{y} at each \mathbf{x} . In other words, we are mapping a uniform grid in the image plane back onto the source plane where we can use this map to locate the images of a particular source. We compare triangles made of nearest neighbors in the image grid mapped onto the source plane to the locations of the sources. If a source point is enclosed by a mapped image triangle, then its image must lie somewhere in that triangle in the image plane, and thus, for any source point, we can locate its image to the uncertainty given by the image grid spacing. One must be careful, though, when considering image triangles that enclose a piece of string because the photon deflection is discontinuous as \mathbf{x} crosses the string. Images in these triangles should be ignored because they represent photons which must pass through the string itself to be observed and are therefore spurious. Since our strings are resolved down to the scale δ , it is natural that the image grid spacing should be δ as well. And, having assumed a self-similar structure for the string, we are free to choose the physical scale that δ represents. For the objects we shall consider for lensing, we find that a good choice for this scale is $\delta/D_l = 0.1$ arc sec.

Using the techniques described above, we shall consider two types of sources, point-like and extended, which will roughly correspond to quasars and galaxies respectively. Let us first consider quasars as they represent what are likely the best objects to look at when trying to observe strings through lensing. Quasars possess a trio of virtues regarding lensing, namely they are high redshift objects ($z \sim 1 - 5$), they are bright and therefore easily observed, and they are typically separated by large enough distances that the chance coincidence of two different quasars being separated at the same scales as typical lensing systems is rare. However, there are a sufficient number to make the observation

of string quasar lensing systems probable (see §II). Quasars are compact, distant, and cannot be spatially resolved with current technology. Thus we shall treat them as idealized point sources. The locations of the resulting images are found as we have described, along with their magnifications which are determined by eq. (35). Figures 4, 5, and 6 show the results quasar lensing with three different segments of cosmic string. In each panel, the source location is shown as a hatched circle, the images as open circles, and the projected string segment as a dashed line. The relative area of the image circles gives the ratios of magnifications of the image to the source. The string is located at a redshift of one and the quasar is located at a redshift of two, while the angular size of each panel is 25 arc sec. The full length of string used in the lensing calculations is not shown, but we use the same segments for the galaxy lenses, and we do show the full segment in figures 7, 9, and 11 respectively. Typical in many of these examples are a number of small demagnified images which reside close to the string itself. These results are qualitatively similar to those one would see if we replaced the string by several point masses with masses similar to the energy in the string. With point masses, The deflection induced by neighboring points cancels around the midpoint between the two masses. Small images tend to form here because the deflection angle changes rapidly around the minima. For strings, it is the kinks and wiggles which provide a similar opportunity. Inside a kink, contributions from different parts of the string can cancel, leading to rapid changes in the deflection. Kinks can also produce small images by just being large concentrations of energy. They produce images in a manner similar to point masses when the source is outside the Einstein ring. The secondary image is smaller and therefore demagnified.

High redshift galaxies also provide interesting candidates for cosmic string lensing, but observing these systems is significantly more challenging. The greatest difficulty lies in observing such objects because they are so faint. Things are further complicated because foreground galaxies may also contaminate the systems making it more difficult to observe the images. Also, typical galaxies are not spherical making it difficult to determine if one is observing a lensing arc or merely an edge on galaxy. However, to qualitatively illustrate a galaxy lensing system, we consider an idealized case of a set of extended spherical sources located at a redshift of $z = 2$, lensed by a string at $z = 1$. The angular size of the sources is 0.5 arc sec which corresponds roughly to the observed size of high redshift galaxies. Seven such sources are scattered randomly in side a $(25 \text{ arc sec})^2$ viewing area mimicking the approximate angular density of real high redshift galaxies [11]. In figures 7, 9, and 11 we show the full string segment used in the lensing calculation along with the sources to be lensed. The dashed box shows the area for which we calculate the images, where outside this region, we expect that the photon deflections will not be particularly accurate due to truncation error. In figures 8, 10, and 12 we show the observed images corresponding their respective sources, and again we note the proliferation of smaller, demagnified images similar to those observed in the quasar images.

VI. CONCLUSIONS

From the results in the previous section, we can see that cosmic strings can produce images which have characteristics unlike the more prosaic galaxy lens. In particular, the proliferation of small demagnified images is a signature that may be unique to long cosmic strings. This suggest the exciting possibility that a cosmic string can be positively identified through gravitational lensing, confirming the existence of these topological defects. Unfortunately, our enthusiasm must be tempered by two important caveats. The first is that these strings are the product of Minkowski space simulations and do not include the effects of the expanding universe. When theses are considered, the structure on the string is stretched so that the fractal dimension falls to approximately $n = 1.1$ [12], so we expect real strings to have smaller kinks and wiggles. The other effect that we ignored is that of gravitational radiation. For loops it is well known that they radiate energy at a rate of $\Gamma G\mu$ where Γ is on the order of 100, so loops shorter than $\Gamma G\mu t$ will have radiated completely away. The effects of gravitational radiation on the structure of fractal strings is not as well understood. An analytic example of a helical string has been calculated by Sakellariadou [13] while the case of small amplitude kinks has been considered by Hindmarsh [14]. Their results suggest that fluctuations on long strings should have a life expectancy of about $d/G\mu$ where d is the typical separation length between kinks—on the same order as the fluctuation. So, one might expect that the strings are straight on scales smaller than $G\mu$ times the horizon scale at the epoch of lensing. For a string located at $z = 1$ this corresponds to an angular scale of 0.5 arc sec, so gravitational radiation may just influence the long string lensing structure. Our examples then represent the most extreme results that one should expect, and real signatures may be less distinct. However, because the small scale structure of our strings is responsible for the demagnified images, we can conclude that gravitational lensing may be a good way to probe that small scale structure. If strings are relatively smooth on the scales we considered in our examples, then any strong lenses observed should produce a pair of undistorted images like those resulting from an infinite straight string. Conversely, if there is significant small scale structure, then one expects to see a number of demagnified images like those seen in the figures.

In §II, we found that quasar–string lensing systems should constitute about 10% to 30% of the observed quasar

lenses, where the rest arise from lensing with galaxies. We suggest that the search for gravitational lenses could on its own confirm or rule out the cosmic string model of structure formation depending on whether such lenses are observed. Since the strings are obviously correlated, a large angle of sky coverage with a large number of quasars is required. In fact, precisely such a survey is currently being developed, namely the Sloan Digital Sky Survey. Some 10^5 quasars with a mean redshift of two are to be observed in a π steradian slice of the sky. We have estimated that one should observe on the order of ten string lenses in the SDSS for an $\Omega = 1$, cosmic string model. The failure to observe any string lensed quasars would require $G\mu < 10^6$, making strings an unlikely candidate for structure formation. Conversely, should a suspected string lens be observed, it is possible to confirm it by looking at galaxy observations in the neighborhood of the lens. With precise observations, one expects to see lensing of high redshift galaxies from nearby parts of the same string. In concert then, quasar observations followed by galaxy observations could provide definitive proof of GUT scale cosmic strings, or rule out cosmic strings as a viable model for the formation of large scale structure.

We would like to thank Tanmay Vachaspati for his help and suggestions. This work was supported with funding from the Department of Energy.

-
- [1] B. Allen *et al.*, Phys. Rev. Lett. **77**, 3061 (1996)
 - [2] J. Magueijo *et al.*, Phys. Rev. **D54**, 3727 (1996)
 - [3] D.P. Bennet and F.R. Bouchet in *The Formation and Evolution of Cosmic Strings*, eds. G.W. Gibbons, S.W. Hawking and T. Vachaspati, (Cambridge University Press 1990).
 - [4] E. L. Turner, J. P. Ostriker and J. R. Gott, Astrophys. J. **284**, 1 (1984)
 - [5] L. M. Krauss and M. White, Astrophys. J. **394**, 385 (1992)
 - [6] A. A. delaix and T. Vachaspati, Phys. Rev. **D54**, 4780 (1996)
 - [7] A. G. Smith and A. Vilenkin, Phys. Rev. **D36**, 990 (1987).
 - [8] T. Vachaspati and A. Vilenkin, Phys. Rev. **D30**, 2036 (1984).
 - [9] See the papers by D.P. Bennet, F.R. Bouchet, N.Turok, A. Albrecht, and, E.P.S. Shellard and B. Allen in *The Formation and Evolution of Cosmic Strings*, eds. G.W. Gibbons, S.W. Hawking and T. Vachaspati, (Cambridge University Press 1990).
 - [10] M. Sakellariadou and A. Villenkin, Phys. Rev. **D42**, 349 (1990)
 - [11] M. J. Sawicki, H. Lin and H. K. L. Yee, Astron. J., **113**, 1 (1997)
 - [12] See *e.g.* F.R. Bouchet in *The Formation and Evolution of Cosmic Strings*, eds. G.W. Gibbons, S.W. Hawking and T. Vachaspati, (Cambridge University Press 1990).
 - [13] M. Sakellariadou, Phys. Rev. **D42**, 354 (1990)
 - [14] M. Hindmarsh, Phys. Lett. **B251**, 28 (1990)

FIG. 1. The probability of a source being lensed by a long cosmic string plotted as a function of source redshift (solid). For comparison, the probability of a source being lensed by a galaxy is shown (dashed).

FIG. 2. A schematic representation of a gravitational lensing system.

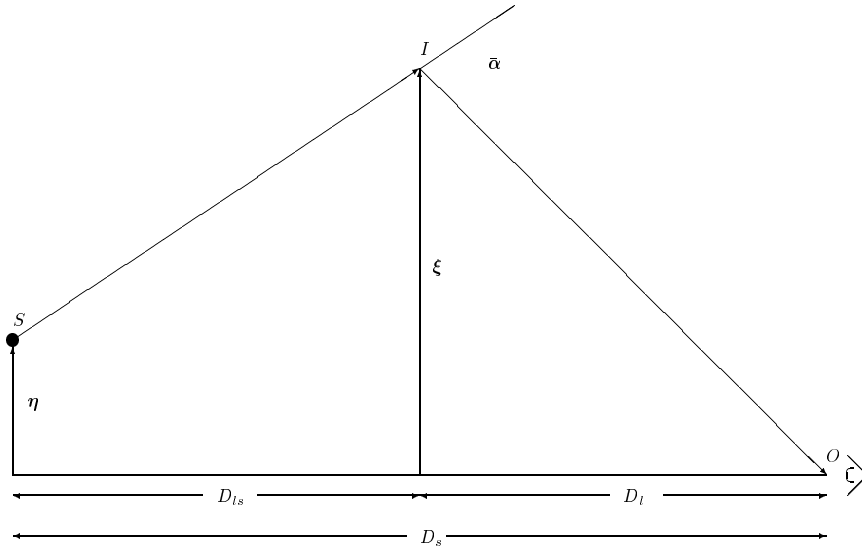


FIG. 3. String conformal length L plotted as a function of point separation distance D . The solid curve is for $t = 0$, the dotted for $t = 256\delta$ and the dashed for $t = 512\delta$. The periodic length of the box is 1024δ .

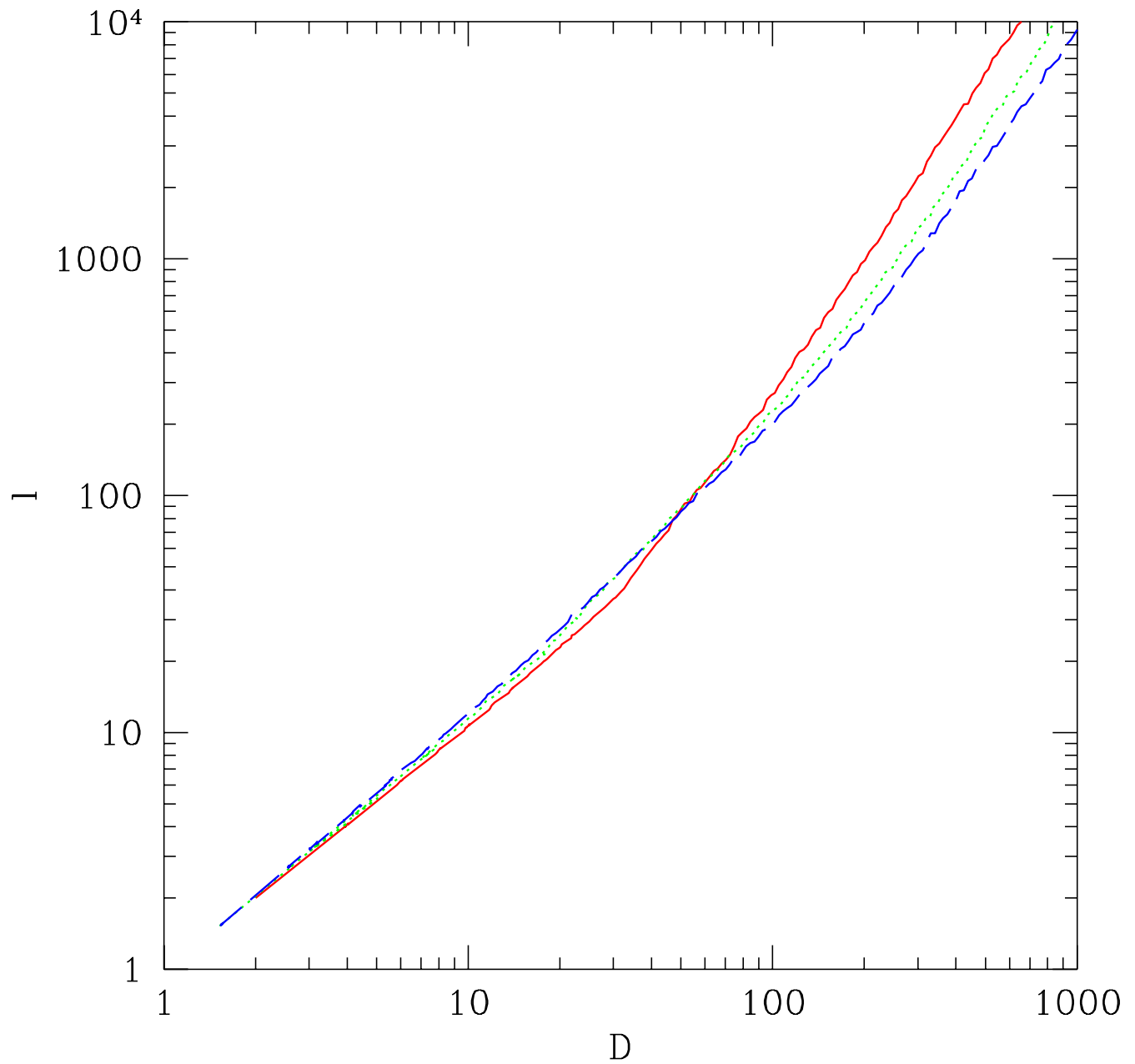


FIG. 4. A string–quasar lensing system. The string is shown as a dashed line while the source is shown as a hatched circle with images shown as open circles. The relative areas are indicative of the magnifications of the images.

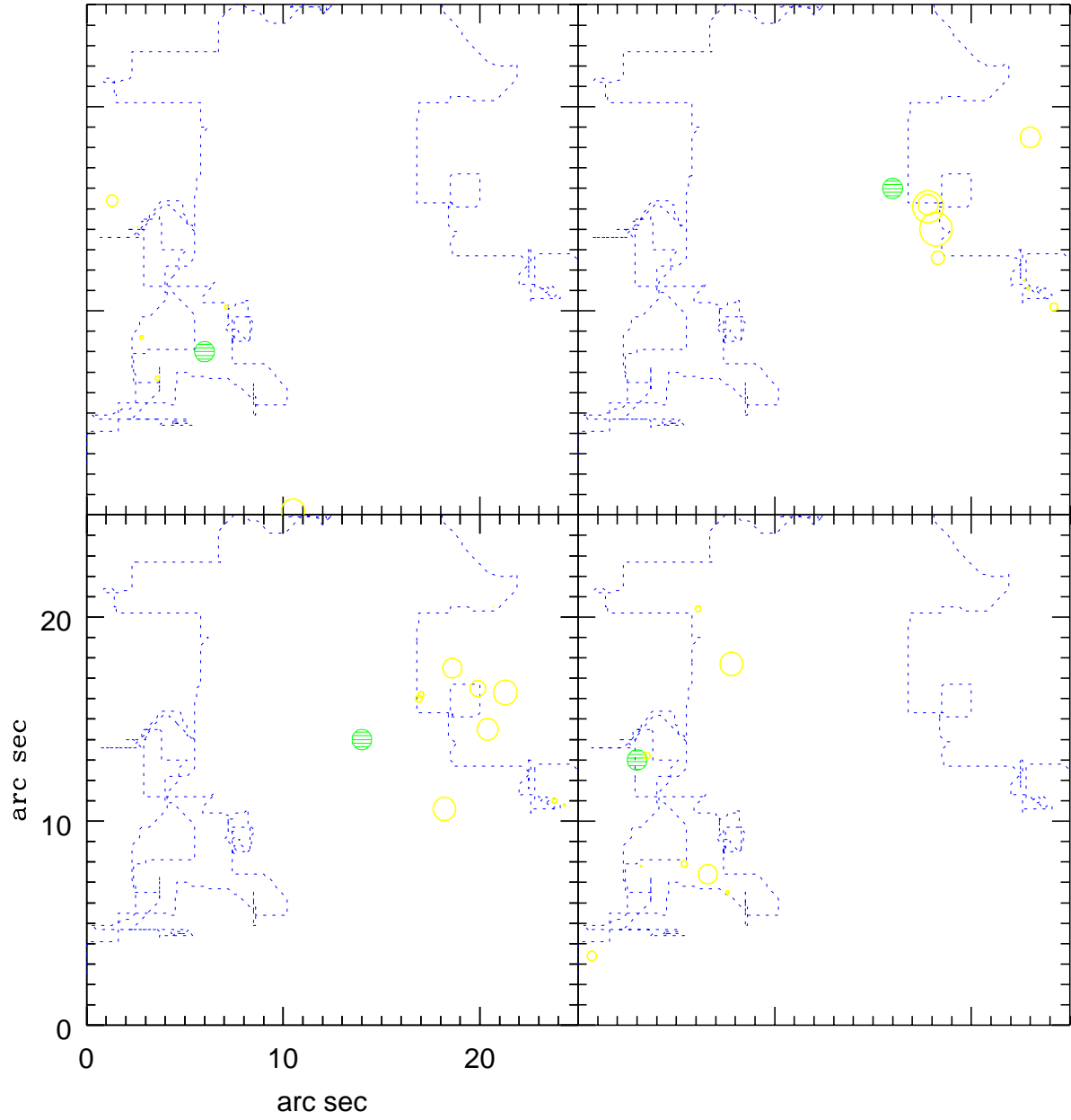


FIG. 5. Same as Fig. 4

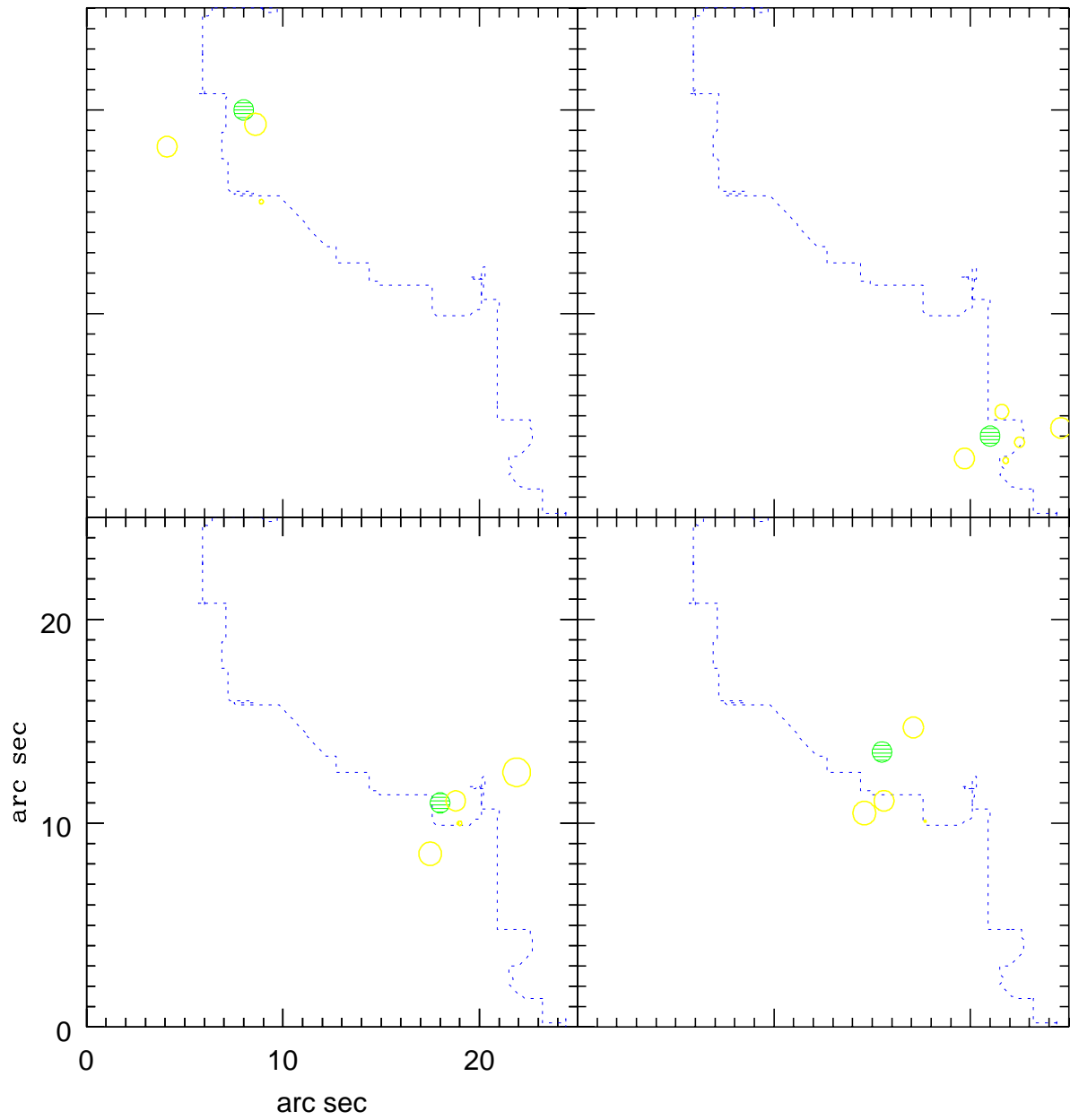


FIG. 6. Same as Fig. 4

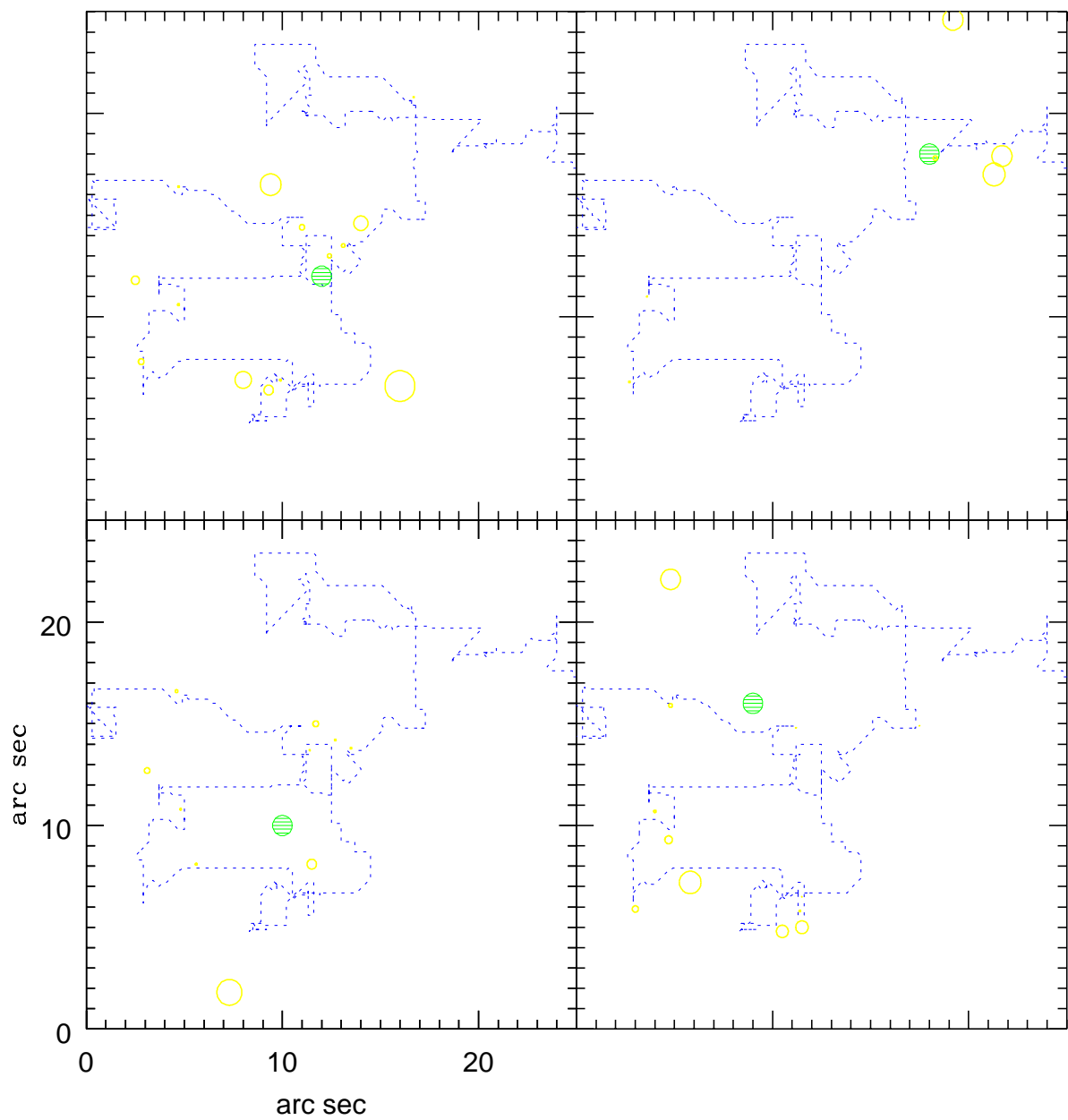


FIG. 8. The images observed for the lensing system shown in Fig. 7

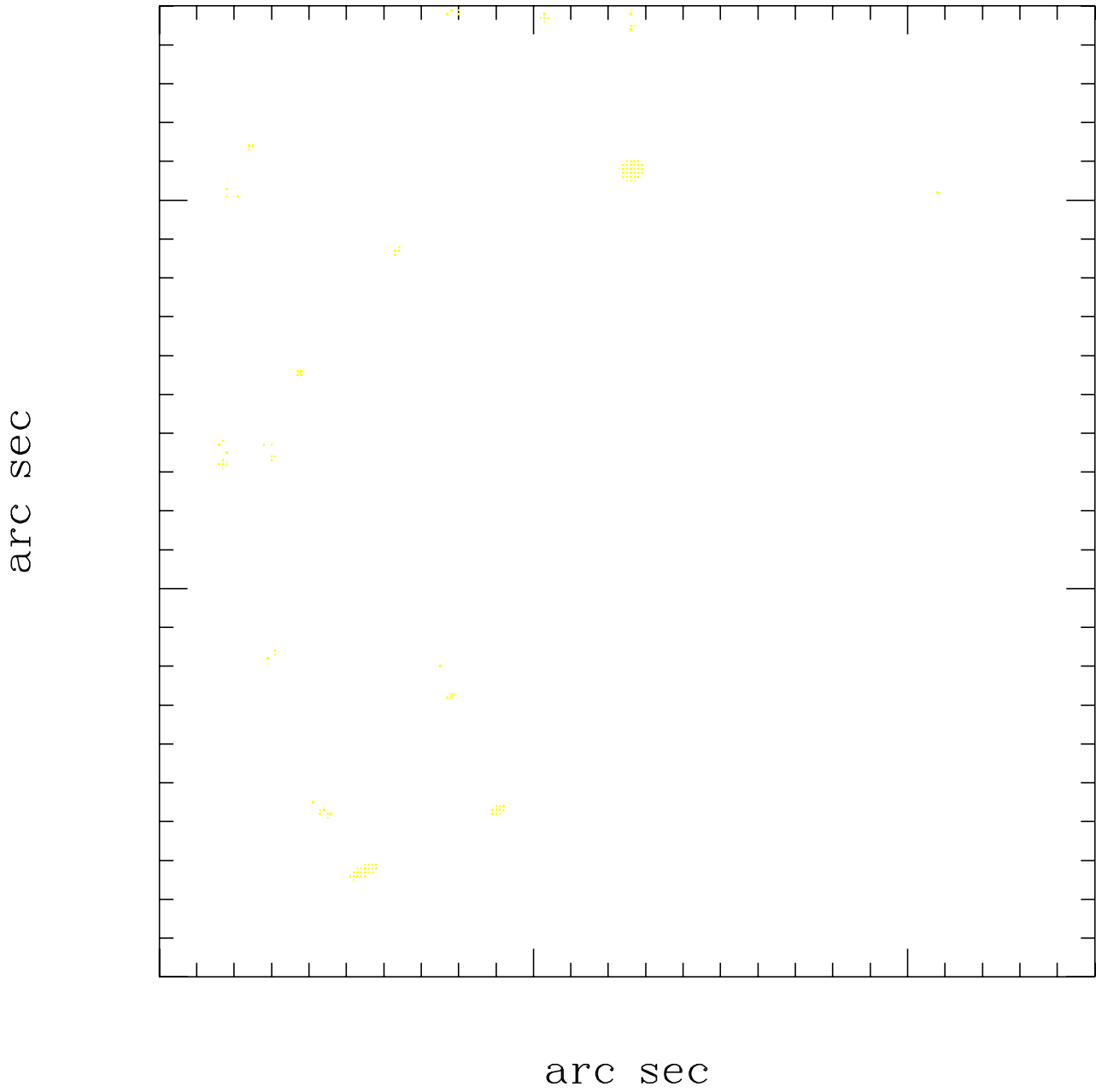


FIG. 10. The images observed for the lensing system shown in Fig. 9

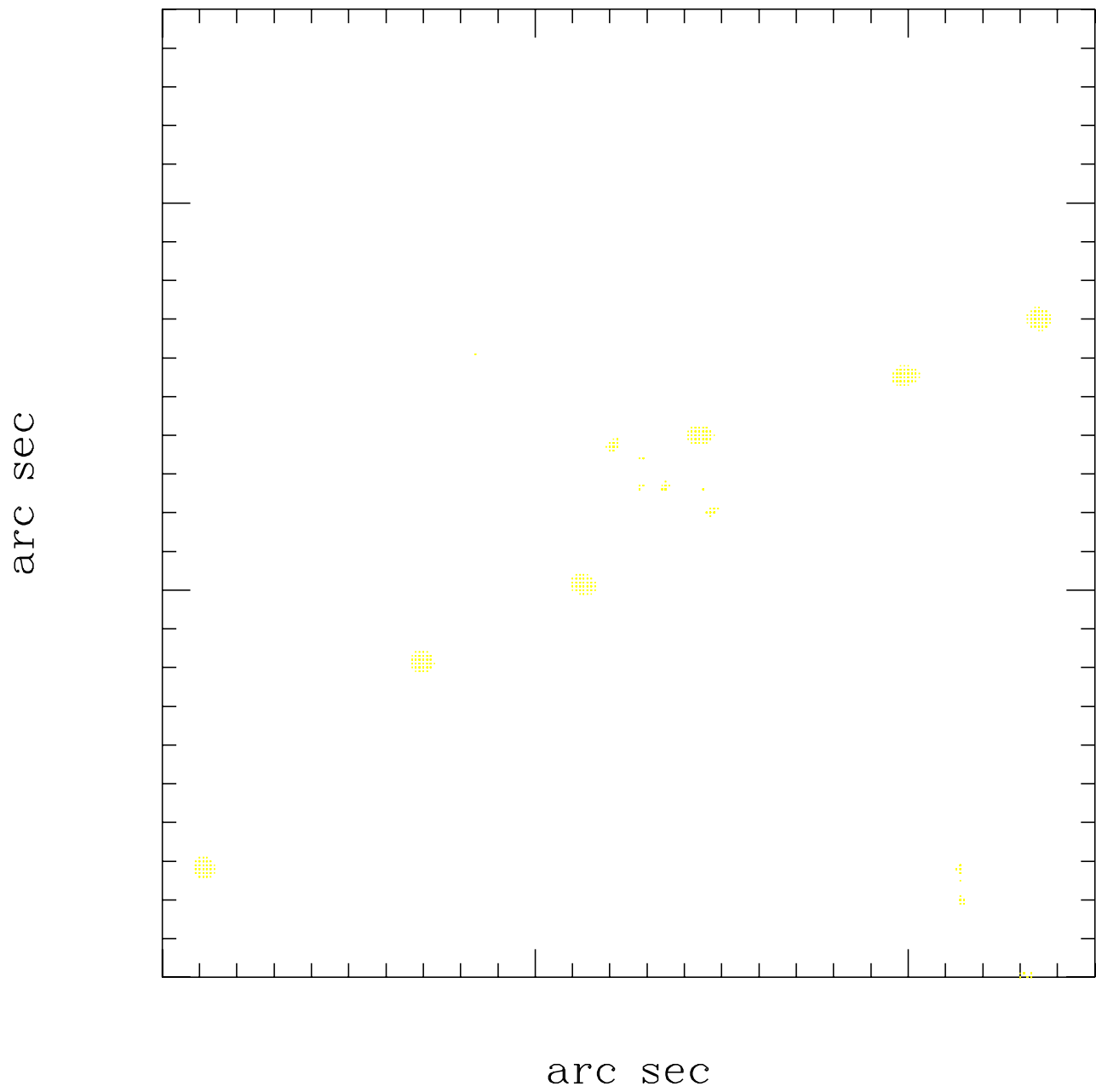


FIG. 11. Another string-galaxy system like Fig. 7

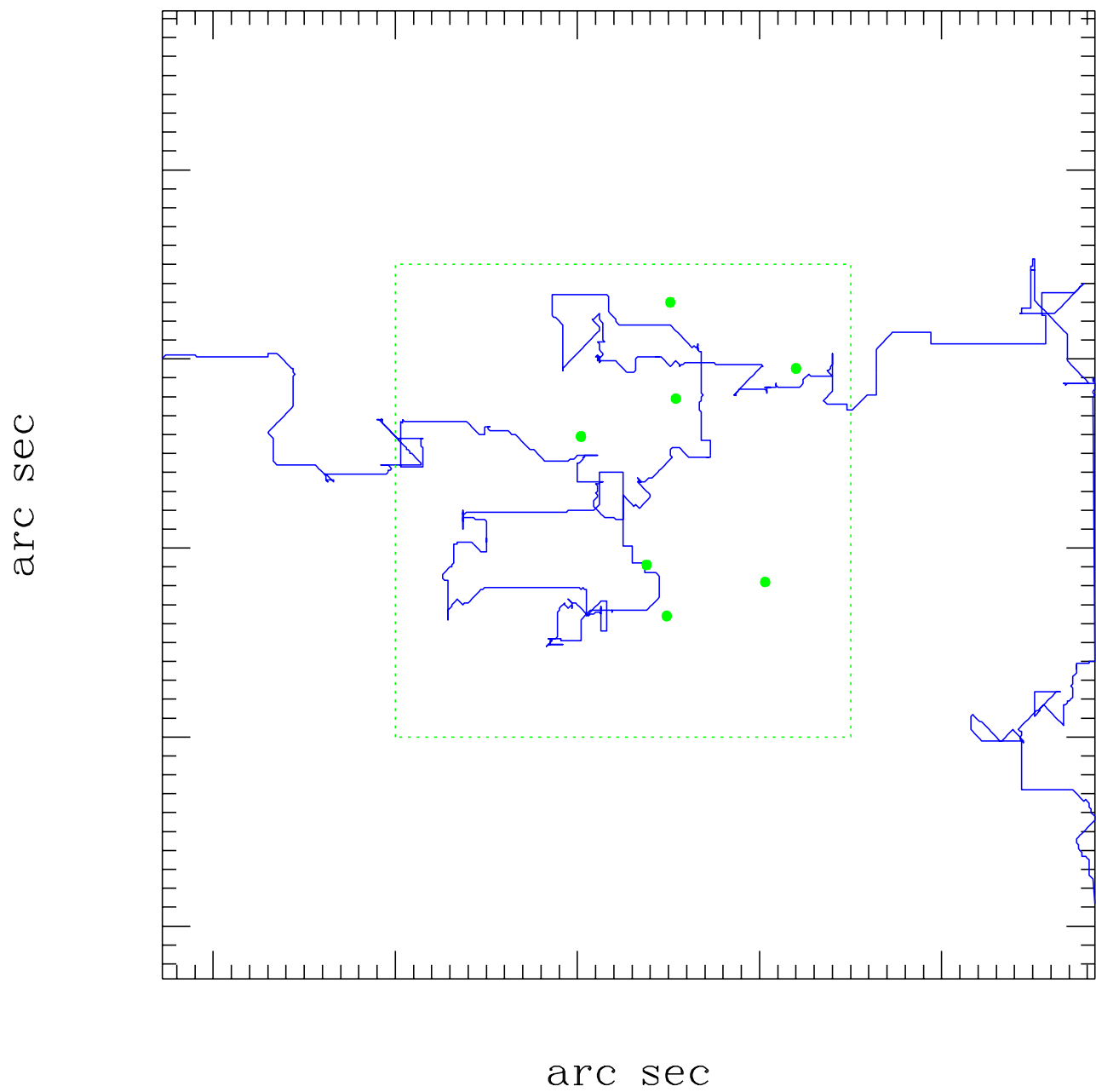


FIG. 12. The images observed for the lensing system shown in Fig. 11

